Dual-Modality Imaging Agents

DOI: 10.1002/ange.201102872

Sequential SPECT and Optical Imaging of Experimental Models of Prostate Cancer with a Dual Modality Inhibitor of the Prostate-Specific Membrane Antigen**

*Sangeeta Ray Banerjee, Mrudula Pullambhatla, Youngjoo Byun, Sridhar Nimmagadda, Catherine A. Foss, Gilbert Green, James J. Fox, Shawn E. Lupold, Ronnie C. Mease, and Martin G. Pomper**

Prostate cancer (PCa) will kill 32000 men in the US this year.[1] Two major issues that contribute to that mortality are: 1) the inability to predict which patients have indolent as opposed to aggressive disease, complicating the choice of appropriate therapy; and, 2) difficulty in assuring a clear surgical margin during prostatectomy. Further complicating management of PCa is the fact that there is no reliable way to image the disease either for the purpose of predicting which tumors may invade and metastasize or for identifying the number of metastatic sites during therapy. Molecular imaging, the non-invasive sensing of cellular and molecular processes in animal models of disease or in patients, can report not only on the anatomy of a tumor, but also on its underlying physiology—possibly predicting its future behavior. Unfortunately, unlike other cancers PCa does not image well with the standard molecular imaging agent, [^{18}F]fluorodeoxyglucose, which can be detected in patients using positron emission tomography (PET).[2] The integral membrane protein prostate-specific membrane antigen (PSMA) is becoming increasingly recognized as a viable target for imaging and therapy of prostate and other forms of cancer.[3–5] PSMA is significantly over-expressed in PCa and metastases, particularly with respect to the hormone-refractory form.[6] PSMA may provide a negative prognostic indicator for PCa—enabling distinction of indolent from aggressive disease.[7]

Dual-modality imaging agents that combine the sensitivity of radionuclide imaging, such as SPECT (single photon emission computed tomography), with the high sensitivity and resolution of NIRF (near-infrared fluorescence) imaging would be useful in the preoperative and intraoperative realms, respectively.[8–10] For staging and preoperative assessment of tumor burden the radionuclide component could initially be used to map disseminated lesions or lesions within the prostate at sub-centimeter resolution. The optical mode could aid in image-guided surgery to delineate tumor margins precisely during and following resection, using a minimally invasive laparoscopic instrument equipped with a NIRF detection system.

Recently, we and others have demonstrated successful PSMA-targeted radiopharmaceutical imaging in experimental models of PCa using cysteine-glutamate or lysine-glutamate ureas.[11–15] With these agents the radionuclide (^{11}C, ^{125}I, ^{18}F) is attached to the cysteine or lysine moiety through a small prosthetic group. For large molecular fragments, such as radiometal (^{99m}Tc, ^{68}Ga) chelators, organic fluorescent molecules, and nanoparticles, we have determined that a linking moiety of at least 20 Å between the large molecule and the lysine moiety is needed.[16–19] We hypothesized that conjugation of a dual (radionuclide and optical) modality imaging platform to a PSMA-targeting urea would enable sequential, dual modality imaging of experimental prostate tumors. Such a dual modality PSMA imaging agent could be used to address each of the two items confounding PCa management described above.

Here we report the first dual modality SPECT/NIRF imaging agent [^{111}In]**1** that demonstrates high and specific uptake in PSMA+ xenografts and pharmacokinetics suitable for targeting PSMA in vivo. The non-radiolabeled compound **1** is prepared conveniently by a combined solid phase and solution phase Fmoc-based peptide synthesis strategy as shown in Scheme 1. Commercially available Fmoc-Lysine-(Boc)-Wang resin was coupled with Fmoc-Lysine(Dde)-OH and DOTA tris(*t*Bu ester)-CO_2H. The resin support was cleaved with a mixture of TFA/CH_2Cl_2/Et_3SiH/H_2O to generate **2**, which also resulted in simultaneous removal of O-*t*Bu and N-Boc groups. Compound **3**,[18] Glu-urea-Lys-linker-NHS, was reacted with the free ε-amine of the lysine of **2** in the presence of DMSO and TEA to generate the urea-DOTA **4** in 60% yield. Removal of the Dde group using 2% hydrazine-hydrate in DMF afforded a free ε-amine that was subsequently conjugated with the commercially available *N*-hydroxysuccinimide ester of IRDye800CW to produce **1**. Compound **1** was labeled with either non-radioactive $^{113/115}$In or radioactive ^{111}In at pH 5.5. The radiochemical yield of [^{111}In]**1** was 60–70%. Compounds were purified by reverse-phase HPLC and characterized by LCMS (Supporting Information). The specific radioactivity of [^{111}In]**1** was 46–

[*] Dr. S. R. Banerjee, M. Pullambhatla, Dr. Y. Byun, Dr. S. Nimmagadda, Dr. C. A. Foss, G. Green, J. J. Fox, Dr. S. E. Lupold, Dr. R. C. Mease, Prof.Dr. M. G. Pomper
The Russell H. Morgan Department of Radiology and Radiological Sciences, Johns Hopkins University
1550 Orleans Street, 492 CRB II, Baltimore, MD 21231 (USA)
E-mail: mpomper@jhmi.edu
Homepage: http://www.hopkinsmedicine.org/pharmacology/research/pomper.html

[**] We thank Dr. David Wasserman of LI-COR Biosciences for use of their equipment and guidance in the in vivo study. We also thank U24 CA92871, R01 CA134675 and K25 CA148901 for financial support. SPECT = single photon emission computed tomography.

Supporting information for this article is available on the WWW under http://dx.doi.org/10.1002/anie.201102872.

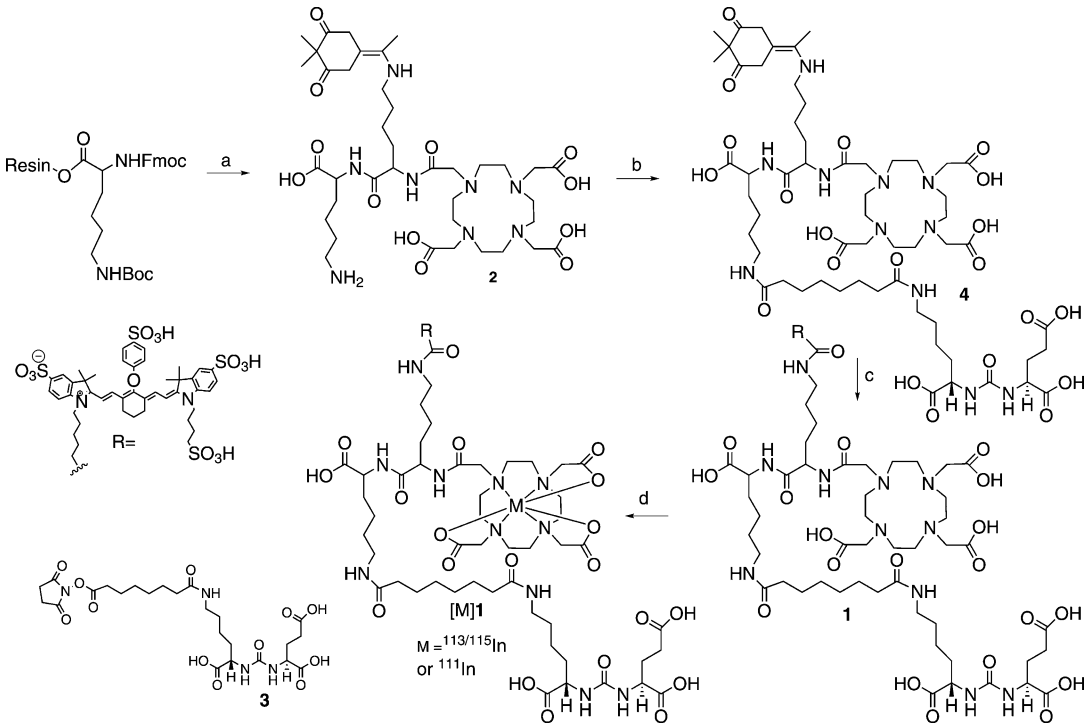

Scheme 1. Synthesis of **1** and [$^{113/115}$In]**1** or [^{111}In]**1**. Reagents and conditions: a) 1. 20% piperidine/DMF; 2. Fmoc-Lys(Dde)-OH, HOBT, HBTU, DIEA; 3. 20% piperidine/DMF; 4. DOTA tris(*t*Bu ester)-OH, HOBT, HBTU, DIEA; 5. TFA/CH_2Cl_2/TES/H_2O (1:1:0.1:0.2), 4 h, RT; b) 3, DMSO, TEA, RT, 3 h; c) 1. 2% hydrazine hydrate/DMF; 2. IRDye800CW-NHS; d) $^{111}InCl_3$ or $^{113/115}In(NO_3)_3$, 200 mM NaOAc, pH 5.5, 40–42 °C, 1 h. HOBT = 1-hydroxybenzotriazole; HBTU = *O*-(benzotriazol-1-yl)-tetramethyluronium hexafluorophosphate, DIEA = ethyldiisopropylamine, DOTA-tris(tert-butylester) = Tri-tert-butyl-1,4,7,10-tetraazacyclododecane-1,4,7,10-tetraacetate , TFA = trifluoroacetic acid, TES = triethylsilane, DMSO = dimethyl sulfoxide, TEA = triethylamine.

325 GBq μmol^{-1}, and the radiochemical purity was ≥ 99%. The electronic spectra of **1** and non-radioactive [$^{113/115}$In]**1** exhibited an absorbance maximum at 776 nm with an extinction coefficient of 181 000 M^{-1} cm^{-1}. We did not observe any significant changes in the spectral properties between **1** and [$^{113/115}$In]**1**. Upon excitation, both **1** and [$^{113/115}$In]**1** provided intense fluorescence with an emission maximum at 792 nm and a fluorescence lifetime of 420 and 483 ps, respectively, in aqueous solution with quantum yields of 8.9% in PBS (phosphate-buffered saline).

PSMA inhibition constant (K_i) values for **1** and [$^{113/115}$In]**1** were determined using a fluorescence-based PSMA inhibition assay.[11] Compounds **1** and [$^{113/115}$In]**1** had K_i values of 0.46 ± 0.05 nM and 1.24 ± 0.07 nM (Supporting Information, Figure S4), respectively, identifying them as potent inhibitors of PSMA with IC_{50} values similar to related compounds employing a single radionuclide chelating or NIRF moiety.[17,19] To determine selectivity and specificity in vitro, PSMA+ PC3-PIP and PSMA− PC3-flu cells were seeded into a 96-well plate containing growth medium and incubated with a serially diluted solution of [$^{113/115}$In]**1** at 4 °C and 37 °C and then washed with PBS. We prefer the isogenic PIP vs flu comparison as the two cell lines are phenotypically identical, differing only in PSMA expression. Figure S5 A shows the lower expression of PSMA within PIP vs. LNCaP, the traditional PSMA + control tumor cell model. NIRF imaging of the 96-well plate showed a dose dependent, PSMA+ cell specific uptake of [$^{113/115}$In]**1** (Figure S6).

Figure 1 shows the pharmacokinetic behavior of [^{111}In]**1** in vivo in severe-combined immune-deficient (SCID) mice bearing both PSMA+ PC3-PIP and PSMA− PC3-flu xenografts.[20] In this experiment 37 MBq of [^{111}In]**1** was administered intravenously (IV) and the animal was imaged repeatedly over a two-day period. Intense radiotracer uptake was seen only in the PSMA+ PIP tumors and in the kidneys. Kidney uptake of the radiotracer is partially due to its route of excretion and to specific uptake from the expression of PSMA in mouse kidneys.[21] To validate the in vivo imaging data, [^{111}In]**1** was also assessed for its pharmacokinetics ex vivo. Table 1 shows the percent injected dose per gram (%ID g^{-1}) of radiotracer in selected organs.

Compound [^{111}In]**1** showed PSMA-dependent binding in PSMA+ PC3-PIP xenografts with rapid accumulation at the tumor site that persisted throughout the course of the experiment. We observed tumor uptake values of 13.9 ± 1.9, 13.3 ± 2.4, 16.4 ± 3.7, 14.6 ± 1.3 %ID g^{-1} (SEM) at 1, 3, 5 and 24 h, respectively. The blood, spleen, gastrointestinal tract, kidney and bladder displayed the highest uptake at 1 h. Steady clearance from the kidneys was demonstrated, from 104.4 ± 9.4 at 1 h to 48.1 ± 17.7 %ID g^{-1} at 24 h. The tumor uptake values of [^{111}In]**1** compare favorably with other low-molecular-weight PSMA imaging agents, including *N*-[*N*-[(*S*)-1,3-dicarboxypropyl]carbamoyl]-4-[^{18}F]fluorobenzyl-L-cysteine ([^{18}F]DCFBC)[15] which has recently been administered to human subjects. PSMA specificity and selectivity of [^{111}In]**1** was further confirmed by effective blocking in PSMA+ PC3

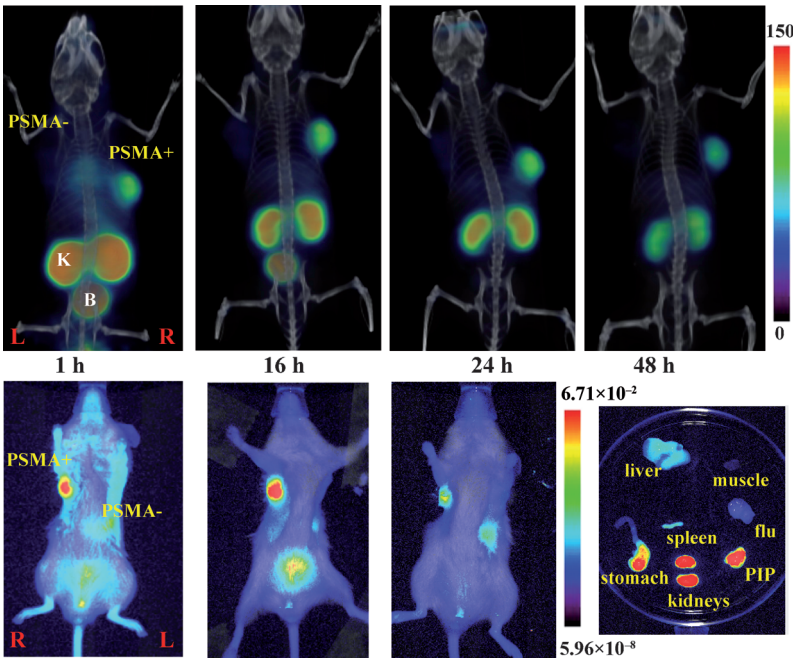

Figure 1. Sequential SPECT-CT (top row) and optical (bottom row) imaging of [^{111}In]**1** using PSMA+ (PIP) and PSMA− (flu) tumors in a male SCID mouse. The mouse was injected intravenously using a single dose of 37 MBq (1 mCi) of [^{111}In]**1** and the uptake was followed until 48 h post-injection. Images of individually harvested organs at 48 h post-injection (bottom right panel). SPECT-CT and optical Images were scaled to the same maximum value (arbitrary units) within their respective modality. K = kidney; B = bladder.

Table 1: Biodistribution (% of injected dose (ID) per gram) of [^{111}In]**1** ($n = 4$).

	1 h	2 h	5 h	24 h
blood	9.9 ± 5.0	7.1 ± 1.2	4.1 ± 0.8	0.9 ± 0.0
heart	3.3 ± 0.5	1.8 ± 0.3	1.8 ± 0.1	0.8 ± 0.1
liver	2.4 ± 0.1	2.2 ± 0.0	3.2 ± 1.2	3.1 ± 0.4
stomach	1.4 ± 0.3	1.2 ± 0.1	2.4 ± 1.8	1.0 ± 0.1
pancreas	2.1 ± 0.1	1.3 ± 0.3	2.0 ± 1.0	1.0 ± 0.3
spleen	11.3 ± 3.7	6.8 ± 0.9	4.8 ± 2.4	8.2 ± 5.4
kidney	104 ± 9.4	97.1 ± 13.0	121.7 ± 21.6	48.1 ± 17.7
muscle	1.2 ± 0.6	0.7 ± 0.2	0.9 ± 0.2	0.4 ± 0.0
sm. int.	1.8 ± 0.5	1.5 ± 0.2	1.6 ± 0.3	2.0 ± 0.7
lrg. int.	1.5 ± 0.5	1.3 ± 0.3	0.8 ± 0.5	2.0 ± 0.4
bladder	4.1 ± 1.7	2.7 ± 1.0	1.1 ± 0.6	2.0 ± 0.5
PC3 PIP	13.9 ± 1.9	13.3 ± 2.4	16.4 ± 3.7	14.6 ± 1.3
PC3 flu	2.1 ± 0.7	2.1 ± 0.5	1.9 ± 0.2	2.0 ± 0.2
PIP:flu	6.7	6.3	8.7	7.4

PIP tumor and kidney (Figure S9) using a dose 50 mg kg^{-1} of the potent, selective PSMA inhibitor *N*-[[[(1S)-1-carboxy-3-methylbutyl]amino]carbonyl]-L-glutamic acid (ZJ43).[22] A significant aspect of this work is the fact that we were able to image PSMA expressing PC3 PIP tumors by SPECT and NIRF sequentially, after using a single injection of [^{111}In]**1**, which was of high specific radioactivity. In so doing we were able to visualize tumor with NIRF imaging after injection of only 0.22 μg (0.1 nmol) of material, which is a tracer dose. For comparison, Table S1 shows clinical studies indicating similar, although somewhat higher, tracer doses of administered radiopharmaceutical. That finding simplifies translation of optical as well as dual modality agents to the clinic because increased safety margins for chemical toxicity are afforded by the low tracer dose. Significantly, since DOTA is a general chelating agent, **1** may also be used with other radiometals such as ^{68}Ga, ^{64}Cu, or ^{86}Y, for PET/optical-based dual modality imaging. Other fluorophore/chelating agent/radiometal combinations can also be envisioned using this approach.

In conclusion, we have developed an efficient chemical and radiochemical synthesis of a dual modality, PSMA-binding compound, which provides sequential imaging by SPECT and NIRF at radiotracer levels. Concurrent, rather than sequential, imaging will be possible with this agent once a corresponding dual modality imaging device becomes available.

Received: April 26, 2011
Revised: June 24, 2011
Published online: August 19, 2011

Keywords: fluorescent probes · imaging agents · prostate cancer · prostate-specific membrane antigen · radiochemistry

[1] A. Jemal, R. Siegel, J. Xu, E. Ward, *Ca-Cancer J. Clin.* **2010**, *60*, 277 – 300.
[2] P. Caroli, C. Nanni, D. Rubello, A. Alavi, S. Fanti, *Indian J. Cancer* **2010**, *47*, 120 – 125.
[3] A. Ghosh, W. D. Heston, *J. Cell. Biochem.* **2004**, *91*, 528 – 539.
[4] M. I. Milowsky, D. M. Nanus, L. Kostakoglu, C. E. Sheehan, S. Vallabhajosula, S. J. Goldsmith, J. S. Ross, N. H. Bander, *J. Clin. Oncol.* **2007**, *25*, 540 – 547.
[5] W. C. Olson, W. D. Heston, A. K. Rajasekaran, *Rev. Recent Clin. Trials* **2007**, *2*, 182 – 190.
[6] N. Schuelke, O. A. Varlamova, G. P. Donovan, D. Ma, J. P. Gardner, D. M. Morrissey, R. R. Arrigale, C. Zhan, A. J. Chodera, K. G. Surowitz, P. J. Maddon, W. D. W. Heston, W. C. Olson, *Proc. Natl. Acad. Sci. USA* **2003**, *100*, 12590 – 12595.
[7] S. Perner, M. D. Hofer, R. Kim, R. B. Shah, H. Li, P. Moller, R. E. Hautmann, J. E. Gschwend, R. Kuefer, M. A. Rubin, *Hum. Pathol.* **2007**, *38*, 696 – 701.
[8] J. Kuil, A. H. Velders, F. W. van Leeuwen, *Bioconjugate Chem.* **2010**, *21*, 1709 – 1719.
[9] H. Lee, W. J. Akers, P. P. Cheney, W. B. Edwards, K. Liang, J. P. Culver, S. Achilefu, *J. Biomed. Opt.* **2009**, *14*, 040507.
[10] R. Chen, J. J. Parry, W. J. Akers, M. Y. Berezin, I. M. El Naqa, S. Achilefu, W. B. Edwards, B. E. Rogers, *J. Nucl. Med.* **2010**, *51*, 1456 – 1463.
[11] Y. Chen, C. A. Foss, Y. Byun, S. Nimmagadda, M. Pullambhatla, J. J. Fox, M. Castanares, S. E. Lupold, J. W. Babich, R. C. Mease, M. G. Pomper, *J. Med. Chem.* **2008**, *51*, 7933 – 7943.
[12] C. A. Foss, R. C. Mease, H. Fan, Y. Wang, H. T. Ravert, R. F. Dannals, R. T. Olszewski, W. D. Heston, A. P. Kozikowski, M. G. Pomper, *Clin. Cancer Res.* **2005**, *11*, 4022 – 4028.

[13] S. M. Hillier, K. P. Maresca, F. J. Femia, J. C. Marquis, C. A. Foss, N. Nguyen, C. N. Zimmerman, J. A. Barrett, W. C. Eckelman, M. G. Pomper, J. L. Joyal, J. W. Babich, *Cancer Res.* **2009**, *69*, 6932 – 6940.
[14] J. L. Joyal, J. A. Barrett, J. C. Marquis, J. Chen, S. M. Hillier, K. P. Maresca, M. Boyd, K. Gage, S. Nimmagadda, J. F. Kronauge, M. Friebe, L. Dinkelborg, J. B. Stubbs, M. G. Stabin, R. Mairs, M. G. Pomper, J. W. Babich, *Cancer Res.* **2010**, *70*, 4045 – 4053.
[15] R. C. Mease, C. L. Dusich, C. A. Foss, H. T. Ravert, R. F. Dannals, J. Seidel, A. Prideaux, J. J. Fox, G. Sgouros, A. P. Kozikowski, M. G. Pomper, *Clin. Cancer Res.* **2008**, *14*, 3036 – 3043.
[16] S. R. Banerjee, C. A. Foss, M. Castanares, R. C. Mease, Y. Byun, J. J. Fox, J. Hilton, S. E. Lupold, A. P. Kozikowski, M. G. Pomper, *J. Med. Chem.* **2008**, *51*, 4504 – 4517.
[17] S. R. Banerjee, M. Pullambhatla, Y. Byun, S. Nimmagadda, G. Green, J. J. Fox, A. Horti, R. C. Mease, M. G. Pomper, *J. Med. Chem.* **2010**, *53*, 5333 – 5341.
[18] S. S. Chandran, S. R. Banerjee, R. C. Mease, M. G. Pomper, S. R. Denmeade, *Cancer Biol. Ther.* **2008**, *7*, 974 – 982.
[19] Y. Chen, S. Dhara, S. R. Banerjee, Y. Byun, M. Pullambhatla, R. C. Mease, M. G. Pomper, *Biochem. Biophys. Res. Commun.* **2009**, *390*, 624 – 629.
[20] S. S. Chang, V. E. Reuter, W. D. Heston, N. H. Bander, L. S. Grauer, P. B. Gaudin, *Cancer Res.* **1999**, *59*, 3192 – 3198.
[21] D. A. Silver, I. Pellicer, W. R. Fair, W. D. Heston, C. Cordon-Cardo, *Clin. Cancer Res.* **1997**, *3*, 81 – 85.
[22] R. T. Olszewski, N. Bukhari, J. Zhou, A. P. Kozikowski, J. T. Wroblewski, S. Shamimi-Noori, B. Wroblewska, T. Bzdega, S. Vicini, F. B. Barton, J. H. Neale, *J. Neurochem.* **2004**, *89*, 876 – 885.

